Proceedings, 7th African Rift Geothermal Conference
Kigali, Rwanda 31st October – 2nd November 2018

Assessment of Carbon Dioxide (CO_2) Partial Pressures in the Menengai Geothermal Area, Kenya

[1]Jeremiah Kipngok, [1]Janet Suwai, [1]Leakey Auko, [1]Sylvia Malimo, [1]George Mulusa, [1]Shilla Chepkemoi and [2]Marini L.

[1]Geothermal Development Company
P.O. Box 17700 – 20100,
Nakuru
[2]Consultant in Applied Geochemistry
Via Antonio Fratti, 253

[1]jkipngok@gdc.co.ke and [2]luigimarini@appliedgeochemistry.it

Keywords

Partial pressure, CO_2, Menengai, groundwater, geochemistry

ABSTRACT

Partial pressure of CO_2 (P_{CO2}) was computed for available analyses of local groundwater within the Menengai geothermal area in order to prepare a unique map of distribution of P_{CO2}. The findings show that variations exist in the distribution of P_{CO2} suggesting that CO_2 is possibly produced by different processes based on the general knowledge of CO_2 geochemistry and $\delta^{13}C$ values of CO_2. The variations in the low P_{CO2} populations are ascribable to processes such as decay of organic matter and root respiration occurring in soils, which are systems exchanging gases with the atmosphere. Elevated P_{CO2} values in the groundwater boreholes suggest deep sources of CO_2 and their geographical distribution further defines tectonic structures that are gas leakage zones within the Menengai area. Further, recent results of $^3He/^4He$ isotope ratio and $\delta^{13}C$ values of CO_2 indicate a mantle origin of the gases in Menengai, with CO_2 showing the possibility of a mixture of a deep (mantle) source and that resulting from thermogenic processes. Future works could focus on carbon isotopic composition ($\delta^{13}C$) of CH_4 to confirm these findings and related hypotheses. Calcite precipitation at T < 193°C could also influence the $\delta^{13}C$ values of CO_2. Additionally, P_{CO2} was equally assessed in the Menengai geothermal reservoir from results of tested wells and shows a wide variation, ranging from about 1 bar to about 50 bars. It is noted from the findings that gas partial pressures can be instrumental in mapping zones where boiling in geothermal wells occur as well as possibly identifying aquifers contributing the highest proportion of gas to the discharge in the case of multiple aquifers in the wellbore, a common occurrence in Menengai. It is proposed that the effects of CO_2 be considered when modelling the Menengai geothermal reservoir.

1. Introduction

Geothermal reservoirs worldwide contain significant amounts of non-condensable gases (NCG) which include CO_2, H_2S, H_2, CH_4, N_2 and NH_3, usually in decreasing order of

importance. CO_2 is the most abundant of these gases hence becoming an important prospecting tool in geothermal exploration. The concentration of this gas in steam vents in geothermal fields ranges from a few tenths of a percent to several percents, although condensation near the surface can result in even higher concentrations. Chiodini et al. (1998) proposed the use of CO_2 flux measurements and P_{CO2} in shallow waters as a permeability indicator in geothermal prospecting to locate geothermal reservoirs of different temperatures. Measuring the diffuse flow of CO_2 through soil in geothermal fields for the purposes of geothermal exploration has increasingly been used in recent years (Chiodini et al., 1998; Fridriksson et al., 2006 and Voltattorni et al., 2010).

Generally, CO_2 produces high-pressure, gas-driven geothermal systems (Haizlip, 2016). Hosgor et al. (2015) notes that the partial pressure of CO_2 (which is linked with the mass fraction of CO_2 in the liquid water through Henry's law) has a considerable role on reservoir performance and energy production. He proposed that when modelling such reservoirs, it is crucial to include the effects of carbon dioxide in the model[1]. If the gas is present in sufficient quantities, it can exert a significant effect on the phase behavior of reservoir fluid (Haizlip, 2016). In the Menengai geothermal field, which is currently under development, CO_2 is the dominant non-condensable gas, accounting for about 3.5% by weight in the steam on average, although varying significantly from well to well, with values as high as ten percent in some of the tested wells.

2. Menengai Geothermal Field

2.1 Background of the Study Area

Menengai geothermal field is one of the recent geothermal prospects to be developed in Kenya. The geothermal field is being developed by Geothermal Development Company (GDC) and currently, production drilling is ongoing after successfully proving steam with the initial wells. The Menengai volcano is located on the floor of the Kenya Rift Valley (Figure 1, left). It is one of the late Quaternary caldera volcanoes in the Kenya Rift Valley, which are asssociated with high thermal gradient as a result of shallow magmatic intrusions.

2.2 Geological Setting

Menengai is largely composed of silica-saturated, peralkaline trachyte, which were believed to be erupted in recent times within the caldera. Leat (1984) divided the exposed rock units in Menengai into pre-caldera, syn-caldera and post-caldera volcanics (Figure 1, right). Tectonically, Menengai is divided into two systems; the Ol'rongai, which has NNW trending faults and is older and the NNE trending Solai system which is younger. Location of drilled wells is shown in Figure 2 while the distribution of groundwater boreholes is given in Figure 4.

[1] The pressure of the gas phase can be usually approximated by simply adding the partial pressure of steam and the partial pressure of CO_2, neglecting the contribution of other gas species.

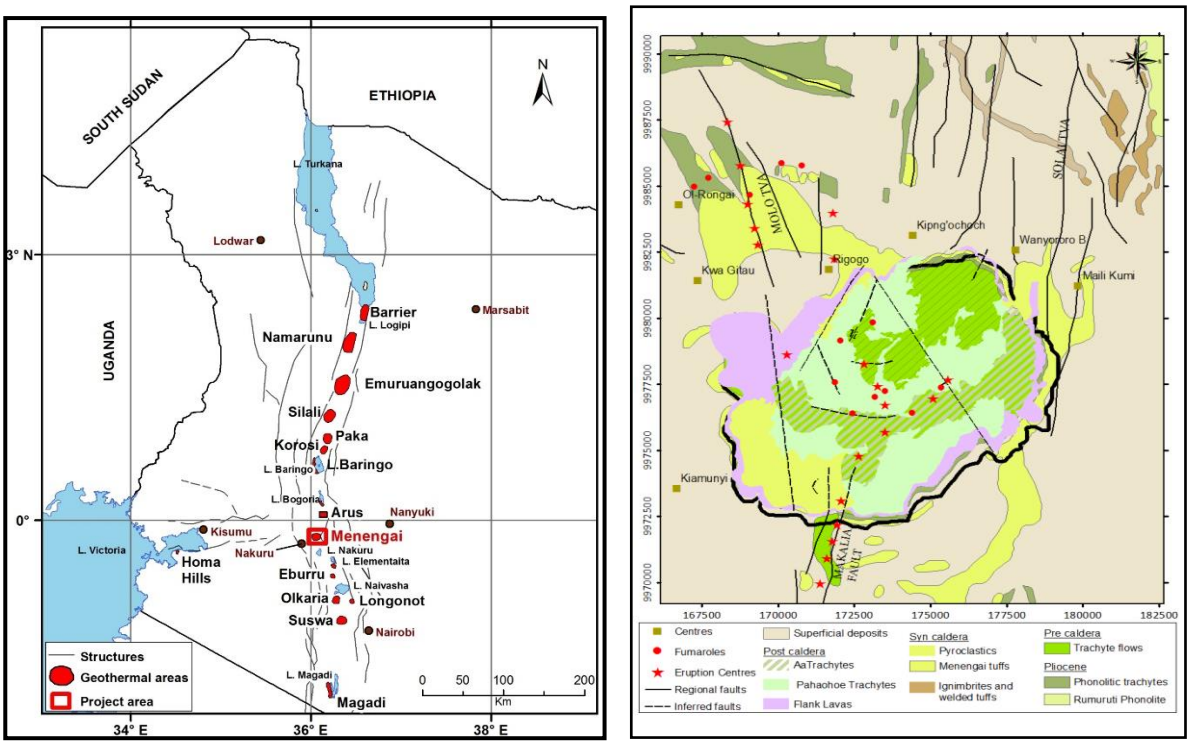

Figure 1: Location of the Menengai geothermal field and other prospects along the Kenya Rift Valley (left; GDC, 2014) and the geological map of the Menengai field and surroundings (right; GDC, 2010).

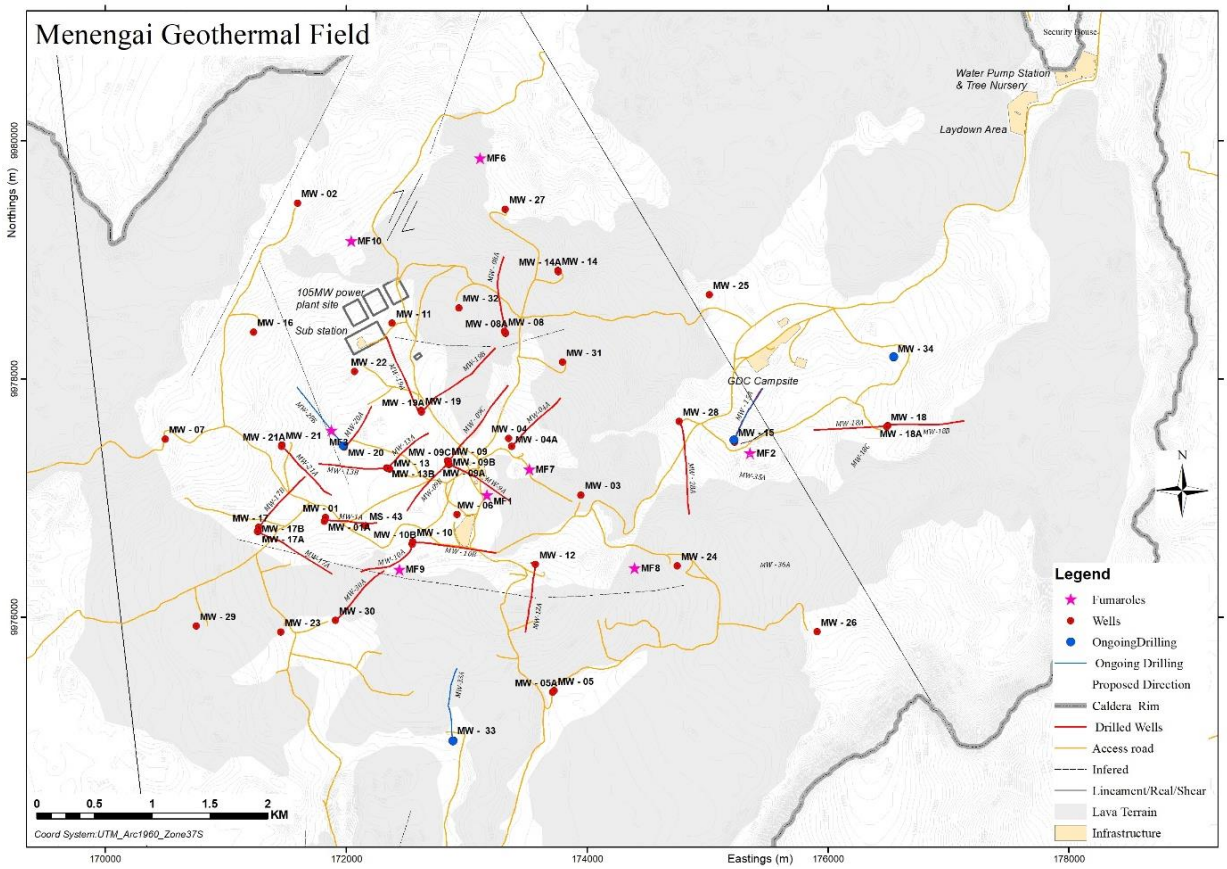

Figure 2: Map showing location of geothermal wells in Menengai (GDC, 2018)

2.3 Distribution of CO_2 Partial Pressure in Groundwater

Chemical and isotopic characteristics of groundwaters from the study area were reported by Geotermica Italiana (1987), GDC (2010) and Malimo (2012). The boreholes sampled by GDC were part of an effort to create a baseline for monitoring possible effects of drilling on groundwater within the project area (Malimo, 2012). Before processing available data, an initial check of their quality was carried out by calculating the charge unbalance, |%dev|. Analyses with |%dev| > 15% were rejected. This rather high threshold was adopted due to the lack of Mg data in the chemical analyses by GDC (2012d), although contents of dissolved magnesium are expected to be relatively low based on the available information. All the samples by Geotermica Italiana (1987) have |%dev| < 7% and were accepted, whereas 11 analyses of GDC (2010) and 185 analyses by GDC (2012d) either have |%dev| > 15% or lack of data for major dissolved constituents (in addition to magnesium).

Partial pressure of CO_2 was then computed for the analyses of the local groundwaters considering, as input data, alkalinity and pH for the Geotermica Italiana analyses, and total inorganic carbon and pH for the GDC analyses. Calculations were carried out taking into account the temperature dependence of the Henry's constant of CO_2, of the dissociation constant of H_2CO_3, and of the dissociation constant of HCO_3^- ion (thermodynamic data from Johnson et al., 1992), whereas activity coefficients of H_2CO_3, HCO_3^- ion and CO_3^{2-} ion were assumed equal to 1.

Initially, P_{CO2} values calculated from GDC analyses and P_{CO2} values computed from Geotermica Italiana analyses were treated separately, constructing two log-probability plots (Figure 3), and separating the individual populations constituting the cumulative distributions through the approach of Sinclair (1974; 1976; 1986)[2]. In this way, it was possible to recognize the presence of four distinct populations in both datasets, whose main statistical parameters are given in Table 1.

Table 1 and Figure 3 show that each population extracted from the GDC dataset compares, within acceptable limits, with the corresponding population separated from the Geotermica Italiana dataset. Therefore, it is possible to consider computed P_{CO2} values altogether and prepare a unique map of distribution of P_{CO2} (Figure 4), without any risk of mixing two different things, such as apples and pears.

Before considering the geographical distribution of P_{CO2} in groundwaters, it is advisable to spend a few words on the characteristics and meaning of individual populations. First, the presence of four individual populations implies that CO_2 is produced by four different processes (sources), whose identification can be attempted based on the general knowledge of CO_2 geochemistry. Nevertheless, inferences should be taken as working hypotheses to be confirmed by use of stable C isotope data.

The low-P_{CO2} populations B, C, and D span the P_{CO2} range 0.0003-0.03 bar. The upper limit of the low-P_{CO2} populations is close to the worldwide maximum soil CO_2 pressure, 0.042 bar (Brook et al., 1983), whereas the lower limit coincides with the average atmospheric P_{CO2}. Therefore, these populations are probably ascribable to processes, such as decay of organic

[2] The probability plot is a simple graphical tool for evaluating the form of the cumulative distribution of a set of numeric data (e.g. Sinclair, 1974, 1976).

matter and root respiration, occurring in soils, which are systems exchanging gases with the atmosphere.

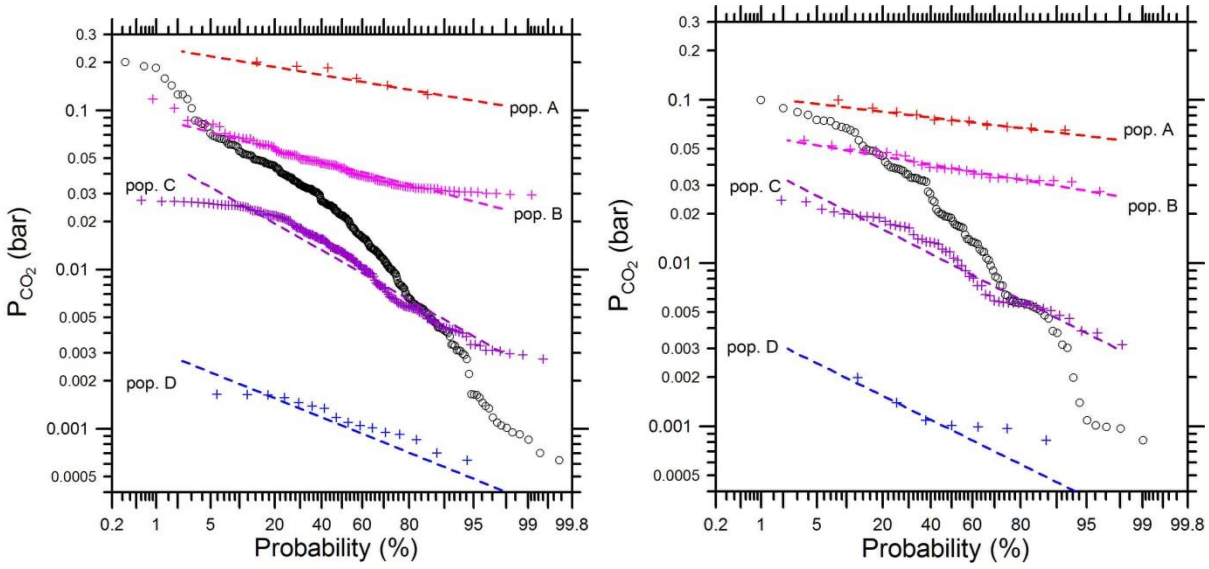

Figure 3: Log-probability plots for the CO_2 partial pressure calculated from GDC analyses (left) and Geotermica Italiana analyses (right) of groundwaters from the study area. In both diagrams, black circles refers to the cumulative distribution of P_{CO2}, whereas red, pink, violet, and blue crosses identify the four individual populations separated adopting the partitioning procedure of Sinclair (1974, 1976, 1986). Computed individual populations are represented by dashed lines using the same colors.

The high-P_{CO2} population A is characterized by P_{CO2} values in the interval 0.06-0.2 bar, which are somewhat above the worldwide maximum soil CO_2 pressure. Consequently, population A is presumably supported by deep CO_2 sources, such as degassing of hydrothermal-magmatic systems, possibly occurring along upflow zones, as well as other processes occurring at depth, such as mantle degassing, exsolution of gases from magma batches, and thermo-metamorphic reactions. Moreover, data on the $\delta^{13}C$ values of CO_2 acquired recently confirm a possible deep origin for this population. In fact, a sample from a hot ground water borehole whose P_{CO2} averages 0.13 bar (from three samples taken over a span of about a year) indicate a mantle source of CO_2 (see section 2.5).

Table 1: Main statistical parameters computed for the four individual populations recognized for CO_2 partial pressure calculated from GDC analyses and Geotermica Italiana analyses

Dataset	Pop.	N	%	Average	Standard dev. (σ)	Median - 2σ	Median	Median + 2 σ
GDC	A	9	3.0	0.162	0.0319	0.108	0.159	0.235
GDC	B	110	36.3	0.0464	0.0144	0.0242	0.0443	0.0813
GDC	C	167	55.1	0.0139	0.0102	0.00302	0.0112	0.0415
GDC	D	17	5.6	0.00117	0.000580	0.000412	0.00105	0.00268
Geotermica Italiana	A	12	12	0.0761	0.0105	0.0572	0.0754	0.0993
Geotermica Italiana	B	28	28	0.0390	0.00767	0.0259	0.0382	0.0565
Geotermica Italiana	C	53	52	0.0117	0.00753	0.00302	0.00982	0.0319
Geotermica Italiana	D	8	7.9	0.00112	0.000697	0.000302	0.000950	0.00299

In the map of Figure 4, most samples belonging to the high-P_{CO2} population A define a NNW-trending tectonic structure, which is situated at a distance of ~6 km from the NE side of the Menengai caldera. This tectonic feature was identified as a steam leakage zone by Geotermica Italiana (1987). Other four samples belonging to the high-P_{CO2} population A, distributed in three widely spaced zones, might define another NNW-trending tectonic structure running close to the western side of the Menengai caldera, although there is a considerable uncertainty on this tectonic feature due to the absence of samples in intermediate position between the high-P_{CO2} zones.

It is however difficult to understand the relations, if any, between these two NNW-trending tectonic structures and the geothermal reservoir hosted in the Menengai caldera. Unfortunately, these anomalies have not been proven through drilling although some of the boreholes located along these structures have elevated discharge temperatures, some in excesss of 50°C (above ambient borehole temperatures of the area).

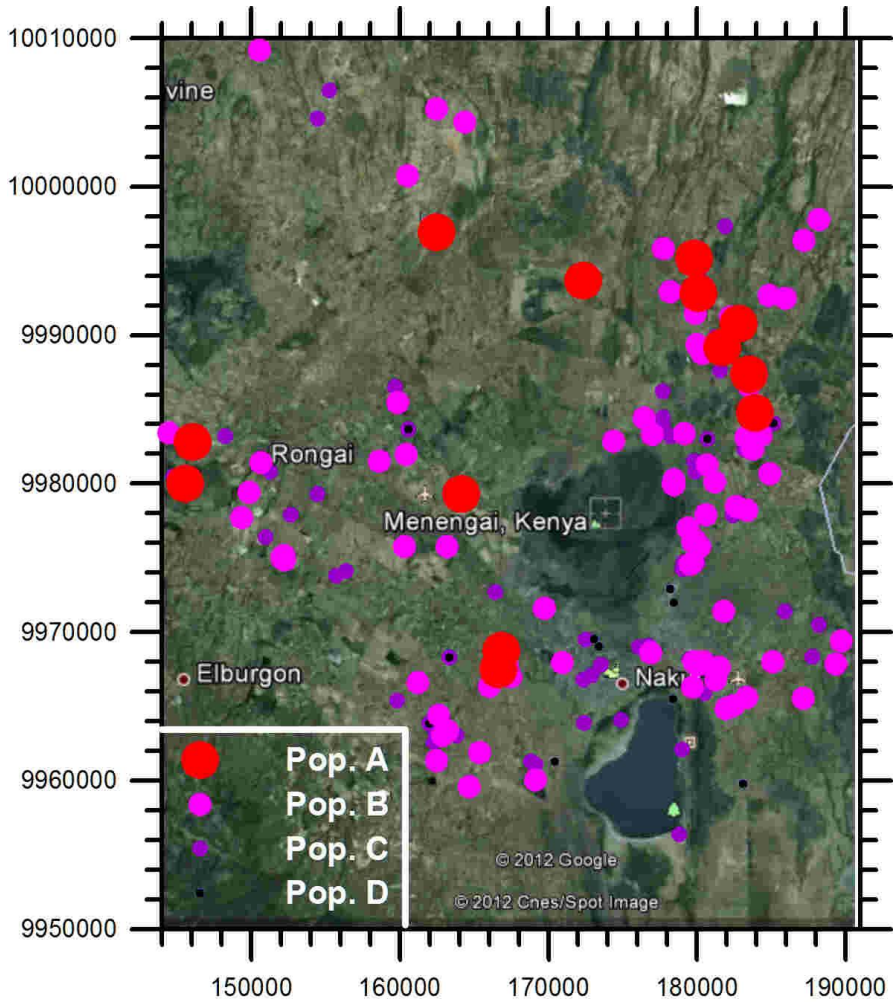

Figure 4: Geographical distribution of PCO_2 in the groundwaters of the Menengai area

2.4 CO_2 Partial Pressure of the Menengai Geothermal Wells

Chemistry data of wells tested since the first well in 2011 was used to calculate the reservoir pH and P_{CO2} by means of a mineral-solution equilibrium model. Geothermal well samples were collected and analyzed as described by Kipng'ok (2011) and Auko (2014).

2.4.1 Evaluation of reservoir pH and PCO_2 through a mineral-solution equilibrium model

Chiodini et al. (1991) investigated the possible geothermometers and P_{CO2}-indicators for aqueous solutions coming from high-temperature (150-300°C) geothermal systems comprising both: (i) low-chloride aqueous solutions of composition from Na-HCO_3-SO_4 to Na-SO_4-HCO_3; (ii) high-chloride brines of Na-Cl composition. These synthetic waters were considered to be in equilibrium with a hydrothermal mineral assemblage made up of albite, K-feldspar, either a Ca-Al-silicate and/or calcite (depending on the P_{CO2}), clinochlore, muscovite, quartz, anhydrite, and fluorite. P_{CO2} was considered an externally controlled parameter fixing the activity of HCO_3^- ion. Chloride was assumed to be a mobile component with molality from 0.003 to 3 mol/kg.

Since the results of Chiodini et al. (1991) cannot be applied to the Na-HCO_3 liquids of the Menengai geothermal field (due to the probable presence of a distinct hydrothermal paragenesis), in this work, the chemistry of the aqueous solution in equilibrium with paragonite, muscovite, clinochlore, calcite, K-feldspar, quartz, and fluorite at variable temperature (175, 200, 225, 250, 275°C), variable P_{CO2} (1, 3, 10, 30, and 100 bar), and fixed Cl and SO_4 concentrations (700 and 200 mg/kg, respectively) was computed by means of the computer code EQ3, which is part of the software package EQ3/6, version 8 (Wolery and Jarek, 2003), using the most recent thermodynamic database (Wolery and Jove Colon, 2007). Results are shown in Table 2.

Table 2: Computed chemistry of the aqueous solution in equilibrium with paragonite, muscovite, clinochlore, calcite, K-feldspar, quartz, and fluorite at variable temperature, P_{CO2} and fixed Cl and SO_4 concentrations of 700 and 200 mg/kg, respectively

T (°C)	pH	PCO_2 (bar)	Na	K	Mg	Ca	Al	F	HCO	CO_2 (HCO_3)	SiO_2
			mg/kg								mg/kg
175	7.3	3	3116	32.4	0.035	0.44	0.5	254	5985	1583	199
175	7	10	5718	58.6	0.171	0.62	0.32	300	1276	5106	195
175	6.8	30	1030	103	0.803	0.92	0.21	342	2485	14577	193
175	6.6	100	1987	192	4.6	1.52	0.12	392	5020	44830	192
200	7.2	3	1843	27.8	0.012	0.41	0.83	172	2894	1694	275
200	7	10	3204	47.9	0.054	0.55	0.55	211	6411	5529	272
200	6.8	30	5633	83.2	0.243	0.82	0.36	249	1279	16028	270
200	6.5	100	1080	156	1.39	1.39	0.23	293	2647	50280	268
225	7.1	3	1212	25.2	0.005	0.42	1.22	113	1410	1863	367
225	7	10	1951	40.3	0.02	0.5	0.85	148	3293	6127	364
225	6.8	30	3286	67.3	0.082	0.72	0.59	180	6780	17964	362
225	6.5	100	6176	125	0.457	1.2	0.38	220	1442	57302	361
250	7.1	3	880	24.2	0.003	0.46	1.58	71.7	670	2094	471
250	6.9	10	1284	35.2	0.008	0.48	1.18	101	1677	6923	469
250	6.8	30	2030	55.2	0.031	0.63	0.85	129	3607	20460	467
250	6.6	100	3667	98.6	0.161	1.01	0.56	166	7922	66157	466
275	7	3	696	24.5	0.002	0.59	1.74	43.7	299	2396	579
275	6.9	10	909	31.8	0.004	0.48	1.42	67.5	814	7950	578
275	6.8	30	1317	45.7	0.013	0.56	1.08	94.4	1859	23630	577
275	6.6	100	2232	76.8	0.061	0.83	0.75	131	4262	77226	576

These data were than processed through multiple regression analysis, obtaining the following relations (concentrations in mg/kg; temperature in K):

$$pH = 5.9133(\pm 0.0511) + \frac{1998.9(\pm 37.6)}{T} - 0.88024(\pm 0.01395).\log(Na) \quad (1)$$

$$\log P_{CO2} = 2.6126(\pm 0.3405) - \frac{4381.1(\pm 250.8)}{T} + 2.1641(\pm 0.09295).\log(Na) \quad (2)$$

The squared regression coefficients are 0.9958 for equation (1) and 0.9696 for equation (2). Equations (1) and (2) were then used to compute pH and P_{CO2} for all the available samples of reservoir liquids, obtaining the average values (and standard deviations) displayed in Table 3.

Table 3: Average pH and P_{CO2} values for the reservoir liquids met by a number of Menengai wells

Well	Discharge Tests Dates	Reservoir pH	P_{CO2}
MW-01	Until May 2012	7.09±0.10	8.4±4.6
	Sept 2012 - November 2012	6.72±0.12	53.2±31.5
	Sept 2013 - April 2014	6.95±0.16	19.1±12.8
	January - April 2015	6.77±0.16	49.5±63.5
MW-01A	October 2014 - March 2015	6.76±0.15	39.6±30.2
MW-03	October 2012 - June 2013	7.47±0.11	1.1±0.6
MW-04	October 2011 - March 2012	7.47±0.11	10.4±4.8
	March - April 2012	7.06±0.16	10.4±8.5
MW-09A	January - March 2015	7.11±0.22	11.7±14.8
MW-12	Until May 2013	7.00±0.26	20.3±24.0
	March - May 2014	6.90±0.29	32.3±31.8
MW-19	April - July 2014	7.30±0.26	2.9±2.8
MW19A	February - April 2015	7.25±0.21	4.2±4.6
MW-20A	December 2014 - February 2015	7.78±0.28	0.3±0.4

Inspection of Table 3 shows that the computed average pH values of reservoir liquids vary over one pH unit approximately, as they range from 6.72 to 7.78. Considering that the pK of water dissociation ranges from 11.5 to 11.2 in the temperature interval of interest (~170 to 280°C), the neutral pH is 5.75 to 5.65. This means that the aqueous solutions of interest have average pH higher than the neutral pH by 1 to 2 pH units. The uncertainties and variations of pH values are relatively small, from 0.1 to 0.3 pH units.

Carbon dioxide partial pressures are characterized by uncertainties and fluctuations larger than pH values and should be taken as educated guesses. In spite of these limitations, it is evident that the reservoir liquids of comparatively low pH (e.g. well MW-01A and well MW-01 in September-November 2012) have relatively high PCO_2 values, whereas the reservoir liquids of comparatively high pH (e.g., wells MW-20A and MW-03) have relatively low P_{CO2} values, as expected.

Reservoir pH was also computed using the WATCH computer code (Arnórsson et al., 1982; Bjarnason, 2010) and the obtained values (not presented in this paper) were 0.52 to 2.25 units higher than the corresponding pH values obtained through the mineral-solution equilibrium model. However, it must be noted that WATCH implicitly assumes that a single reservoir zone contributes to production while in contrast to this assumption, fluids are contributed to the Menengai wells from different feed zones. These significant differences in pH are due to the fact that, on the one hand, pH values calculated by WATCH are controlled by partitioning

of gases (chiefly CO_2) between coexisting vapor and liquid phases whereas, on the other hand, pH values estimated through the mineral-solution equilibrium model are consistent with the presence of a single liquid phase in which gases are entirely dissolved. These pH differences are expected, considering that WATCH results refer to in-hole conditions, whereas the mineral-solution equilibrium model provides hints on the conditions prevailing in the aquifers of the unperturbed reservoir, acting as feed zones, but sufficiently far from the entrance into the borehole.

Not surprisingly, the logarithms of CO_2 partial pressures computed by WATCH are 0.27 to 1.89 log-units lower than the corresponding log P_{CO2} values obtained through the mineral-solution equilibrium model. Moreover, the absolute values of the differences in log P_{CO2} values are similar and strictly related to the corresponding absolute values of the differences in pH values, as summarized by the following relation:

$$\triangle \log PCO_2 = 0.936.\triangle pH - 0.0519 \quad (R^2 = 0.886) \qquad (3)$$

This fact is in line with the pivotal role of CO_2 in controlling the pH of the liquid phase both under natural reservoir conditions and in the borehole.

2.4.2 Effects of P_{CO2} on boiling in Menengai wells

Carbon dioxide has the tendency to shift the flashing point of the reservoir fluid to a considerably higher value and causes a gas phase to form in the reservoir (Hosgor et al., 2015). Kipng'ok (2011) evaluated the effect of high gas pressures (predominantly CO_2) in Menengai well MW-01 and the effect on the boiling point of the water is also evident, the gas pressures lowering the boiling point of water in the well and causing boiling to occur at a higher pressure, that is, deeper in the well. The present work extends the assessment to other geothermal wells in Menengai. Calculated pressure for pure water at different temperatures and the measured down-hole pressure during discharge for ten wells have been plotted and presented in Figure 5. Significant concentrations of CO_2 in the wells discharge made possible the use of CO_2 partial pressures to map zones of fluid inflows and boiling in the wells. Zones showing significant lowering of the boiling point (increase in pressure) could imply increase in gas. In well MW-01 for example, the gas content (CO_2) in the well discharge increased significantly when the fluid from deeper aquifers was cut off by a blockage (possibly calcite deposits) at around 1800 m depth. This suggests that the shallower feeders have higher CO_2 and the shift in the flashing point is evident in graph 1 of Figure 5. As Hosgor et al. (2015) proposes, it is therefore important to consider the effects of carbon dioxide when modeling the Menengai reservoirs due to significant CO_2 content.

Notably though, most wells in Menengai are characterized by 'excess' discharge enthalpy (higher than that of vapor-saturated liquid at the aquifer temperature), and in some cases very pronounced, owing to reservoir boiling and preferential steam inflow into the well. In such wells, this approach is not applicable, like what is seen in the graph of MW-18A and more so in single phase steam wells.

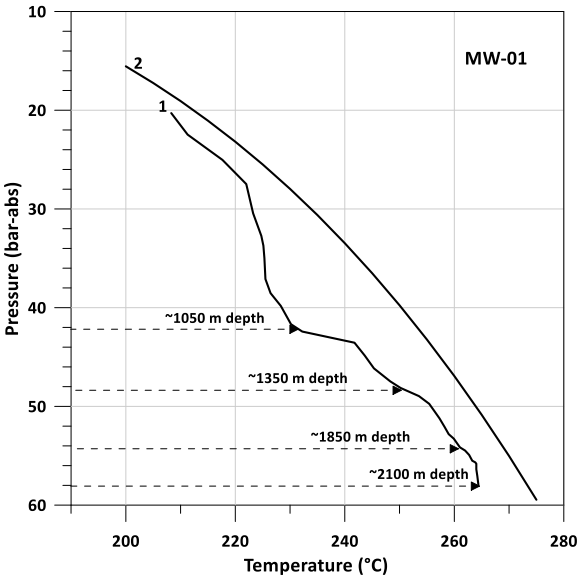
MW-01
Pressure (bar-abs)
Temperature (°C)
~1050 m depth
~1350 m depth
~1850 m depth
~2100 m depth

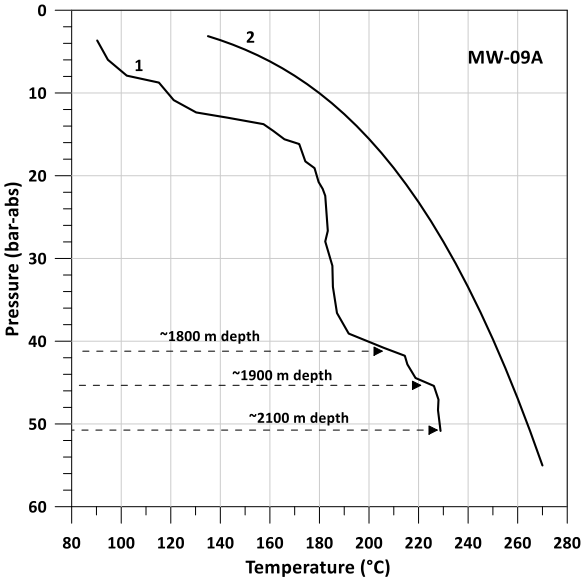
MW-09A
Pressure (bar-abs)
Temperature (°C)
~1800 m depth
~1900 m depth
~2100 m depth

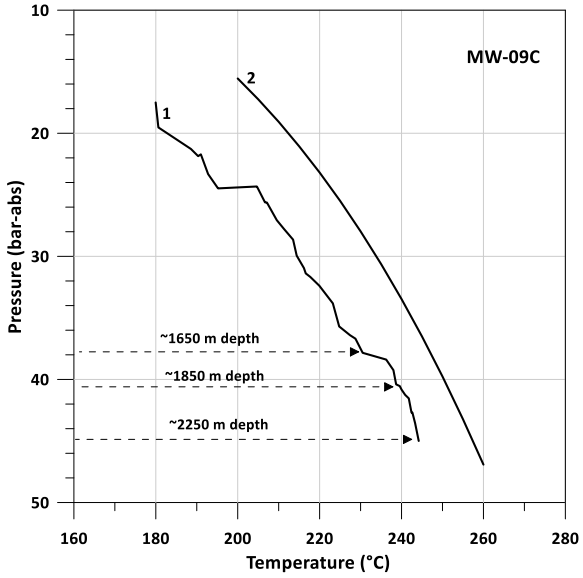
MW-09C
Pressure (bar-abs)
Temperature (°C)
~1650 m depth
~1850 m depth
~2250 m depth

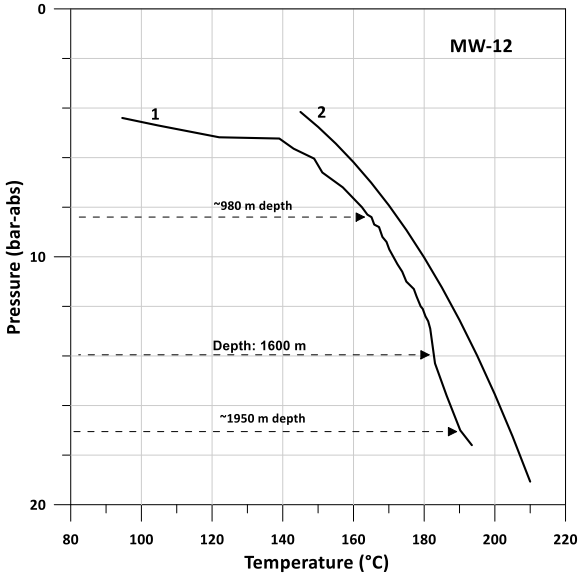
MW-12
Pressure (bar-abs)
Temperature (°C)
~980 m depth
Depth: 1600 m
~1950 m depth

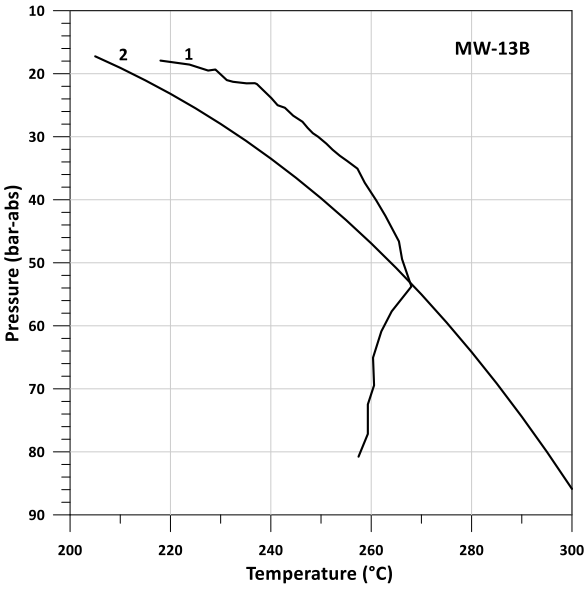
MW-13B
Pressure (bar-abs)
Temperature (°C)

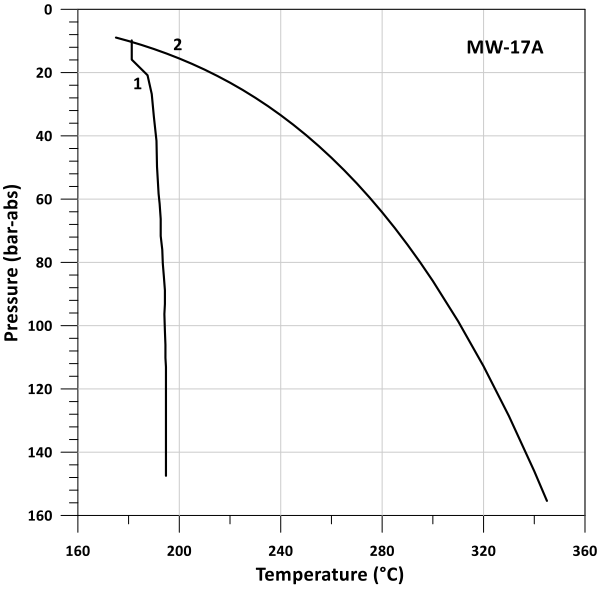
MW-17A
Pressure (bar-abs)
Temperature (°C)

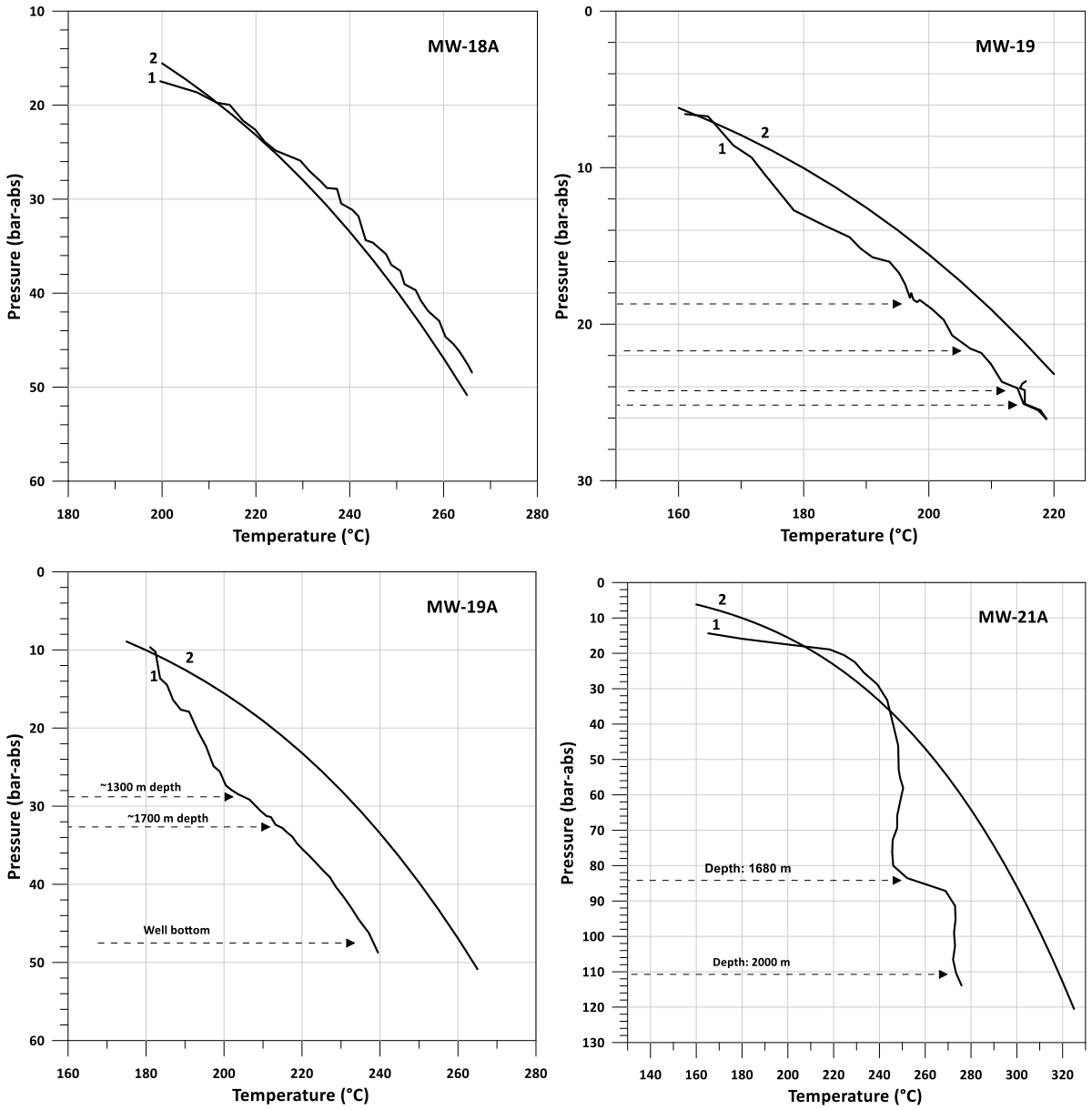

Figure 5: Pressure at measured and calculated temperatures. Curve 1: Measured temperature and pressure (hydrostatic) during discharge of the wells; Curve 2: Temperature and pressure of saturated vapor for pure H_2O. Arrows indicate possible aquifers (modified from Kipng'ok, 2011).

2.5 $\delta^{13}C$ values of CO_2

Recent works in Menengai included determination of $^3He/^4He$ isotope ratio and $\delta^{13}C$ value of CO_2 in geothermal wells and a ground water borehole (DIC) located to the west of Menengai caldera that discharges at an elevated temperature of 57°C (Figure 6). All the samples were collected in January 2018 except for well MW-18A (highlighted in purple) which was collected in May 2017 during the testing of the well. It is important to note that most of the wells were sampled during shut in and could be a factor in explaining the observed results.

Preliminary inferences from available results of $^3He/^4He$ isotope ratio and $\delta^{13}C$ value of CO_2 suggest a deep (mantle) origin of the gases. The $\delta^{13}C$ value of CO_2 in Menengai geothermal wells fluids however is generally lighter (ranging from -5.9 to -16 ‰) and could possibly be the result of mixing between of deep CO_2 (from the mantle) with CO_2 produced by thermogenic decomposition of organic matter. It is likely that this process could be

responsible for the CH_4 content in the fluids discharged by Menengai geothermal wells, which vary significantly in the different parts of the geothermal field, ranging from 0.7 to 56 mmol/kg. Further, studies in the Kenya rift (KRV) indicate that hydrocarbon values are consistent with their thermogenic origin from decomposition of organic matter (Allen and Darling, 1992; Darling et al., 1995; Darling, 1998). However, determination of carbon isotopic composition of CH_4 in future works is recommended so as to prove this postulation.

Calcite precipitation at temperatures lower than 193°C could also be invoked to explain the comparatively low $\delta^{13}C$ values of CO_2. In fact, the calcite-CO_2 fractionation factor is positive below 193°C, is nil at this temperature, and is negative above 193°C (data from Ohmoto and Rye, 1979). Therefore, at temperatures lower than 193°C, precipitating calcite is enriched in ^{13}C and the remaining dissolved carbon species are depleted in ^{13}C.

Notably, it is difficult to distinguish any influence of atmospheric air on the samples because the $\delta^{13}C$ signature of atmospheric CO_2 appear to overlap that of magmatic CO_2 (Figure 7).

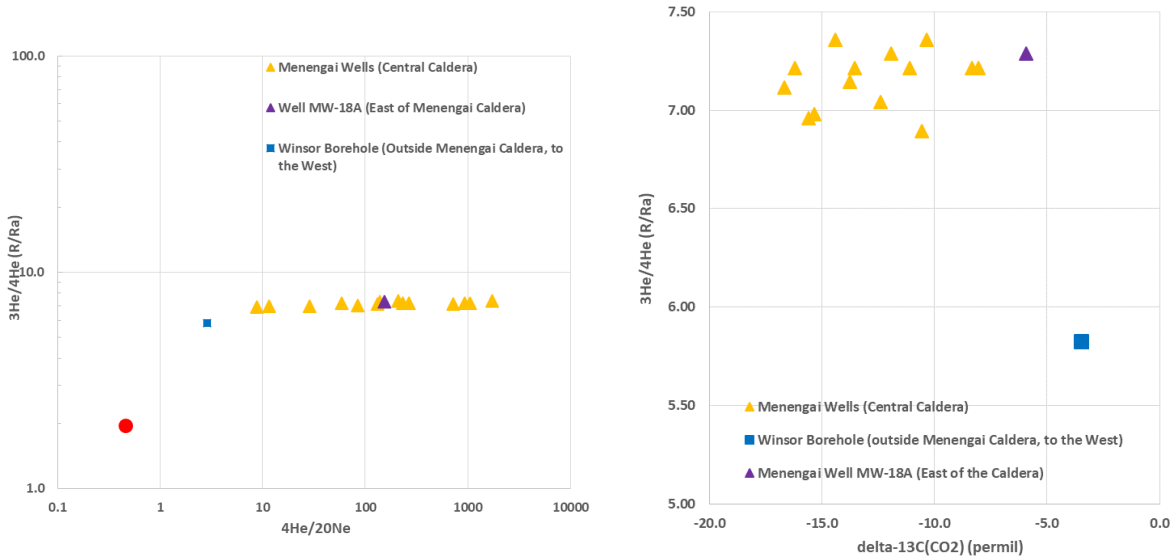

Figure 6: $^3He/^4He$ (R/R_A) against $^4He/Ne$ (left) and $^3He/^4He$ (R/RA) against $\delta^{13}C$ of CO_2 (right)

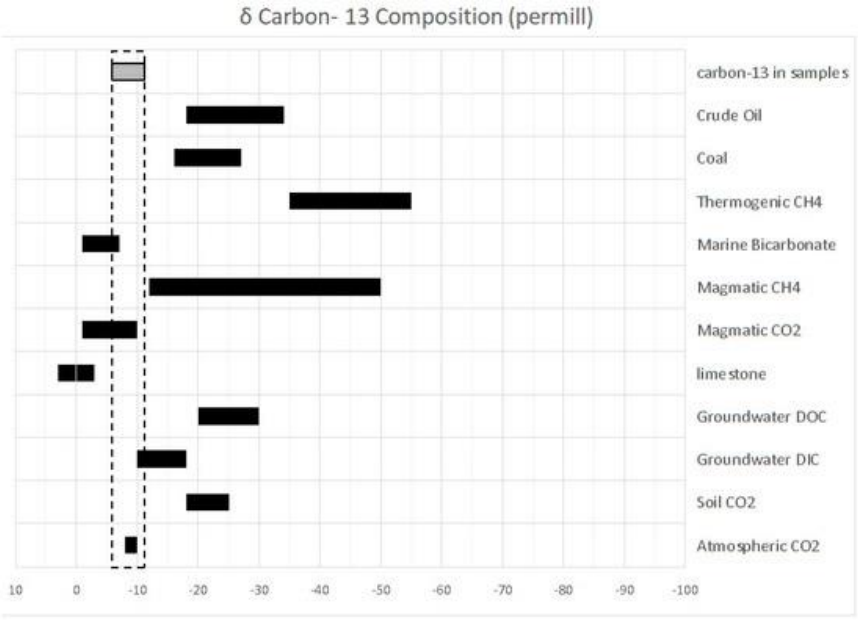

Figure 6: Variation in $\delta^{13}C$ of CO_2 of different origins (Iskandar et al., 2018; the dotted boxed area represents the range of $\delta^{13}C$ of CO_2 values for Tampomas Volcano fluid samples).

3. Conclusion

The following inferences and recommendations are made from the findings on assessment of CO_2 partial pressure in the Menengai geothermal area:

- Carbon dioxide partial pressure in boreholes can be an important prospecting tool, especially where there is sufficient distribution, to map structures as is evident in the Menengai geothermal area findings. This could be complimented by CO_2 flux measurements. Unfortunately, these anomalies have not the proven through drilling.
- The presence of CO_2 in significant proportions in the NCG in Menengai geothermal fluids considerably affects boiling and phase conditions in geothermal reservoirs and wells.
- The main origin of CO_2 in Menengai is the mantle with a possible contribution from thermogenic processes and a possible influence of calcite precipitation at T < 193°C.
- Future works in Menengai could focus on $\delta^{13}C$ values of CO_2 and CH_4 to confirm the postulated contribution of thermogenic process to the NCG.
- Considering the significant effect of CO_2 in Menengai geothermal wells, modelling of the Menengai reservoir should factor in the effects of carbon dioxide in the model.

REFERENCES

Allen D.J. and Darling W.G. "Geothermics and the hydrogeology of the Kenya Rift Valley between Lake Baringo and Lake Turkana." *British Geological Survey Research Report* SD/92/1 (1992).

Arnórsson, S., Sigurdsson, S., and Svavarsson, H. "The chemistry of geothermal waters in Iceland: I. Calculation of aqueous speciation from 0° to 370 °C." *Geochim. Cosmochim. Acta* 46 (1982), pp. 1513–1532.

Auko, L.O. "Evaluation of Fluid mineral interaction in the Menengai geothermal system, Central rift-Kenya. UNU-GTP publications, Report 8 (2014).

Bjarnason J.Ö. "The chemical speciation program WATCH, version 2.4. User's guide." *Iceland Water Chemistry Group*, ÍSOR, Reykjavik (2010), 9 pp.

Chiodini et al. Chiodini G., Cioni R., Guidi M., Marini, L. "Chemical geothermometry and geobarometry in hydrothermal aqueous solutions: A theoretical investigation based on a mineral-solution equilibrium model." *Geochim. Cosmochim. Acta*, 55 (1991), 2709-2727.

Chiodini G., Marini L. "Hydrothermal gas equilibria: The H_2O-H_2-CO_2-CO-CH_4 system." *Geochim. Cosmochim. Acta* 62 (1998), 2673-2687.

Darling W.G. "Hydrothermal hydrocarbon gases: 2, Application in the East African Rift System." *Appl. Geochem* (1998). 13: 825 - 840.

Darling W.G., E. Griesshaber, J.N. Andrews, H. Ármannsson, and O'Nions, R.K. "The origin of Hydrothermal and other gases in the Kenya Rift Valley." *Geochim. Cosmochim. Acta* 59 (1995): 2501 - 2512

Fridriksson T., Kristjánsson, B.R., Ármannsson, H., Margrétardóttir, E., Ólafsdóttir S., Chiodini G. (2006) "CO_2 emissions and heat flow through soil, fumaroles, and steam heated mud pools at the Reykjanes geothermal area, SW Iceland. Appl. Geochem., 21, 1551– 569.

GDC. “Menengai Geothermal Prospect. A Geothermal Resource Assessment Project Report.” Second Edition (2010).

GDC. “Kenya geothermal prospects map.” *GDC Database* (2014).

GDC. “Map of Menengai caldera showing location of geothermal wells.” *GDC Database* (2018).

Geotermica Italiana Srl. “Geothermal Reconnaissance Survey in the MenengaiBogoria area in the Kenya Rift Valley.” UN*(DTCD)/GOK* (1987), Volume V –Geochemistry.

Haizlip, J., Stover, M.M.,Garg,S.K., Tut Haklıdır, F.S and Prina, N. “Origin and Impacts of High Concentrations of Carbon Dioxide in Geothermal Fluids of Western Turkey.” *Proceedings, 41st Workshop on Geothermal Reservoir Engineering* Stanford University, Stanford, California (2016), February 22-24.

Hosgor et al. “Effects of Carbon Dioxide Dissolved in Geothermal Water on Reservoir Production Performance.” *Proceedings World Geothermal Congress 2015*, Melbourne, Australia (2015), 19-25 April.

Iskandar, I., Dermawan, F.A., Sianipar J.Y., Suryantini and Notosiswoyo S. “Characteristic and Mixing Mechanisms of Thermal Fluid at the Tampomas Volcano, West Java, Using Hydrogeochemistry, Stable Isotope and ^{222}Rn Analyses.” *Geosciences* (2018), 8(4), 103, 21 March 2018.

Kipng’ok, J. “Fluid chemistry, feed zones and boiling in the first geothermal exploration well at Menengai, Kenya.” *UNU-GTP publications,* Report 15, (2011), 281-302.

Leat, P.T. “Geological evolution of the trachytic volcano Menengai, Kenya Rift Valley.” *J Geol Soc* London, 141, (1984), 1057-1069.

Malimo, S.J. “Creation of a Geohazard Monitoring Baseline for the Menengai Geothermal Field. Proceedings, ARGeo C3 conefrence, Nairobi, Kenya (2014).

Mehrtens, M.B. Sinclair A.J. & Thompson I. Eds. Society of Economic Geologists, ElPaso. Rewiews in Economic Geology, 3, 97-115.

Ohmoto, H., Rye, R.O. “Isotope of sulfur and carbon. In: Geochemistry of Hydrothermal Ore Deposits.” *H.L. Barnes* Ed., Wiley, 2nd Edition, (1979), pp. 509-567.

Sinclair A.J. “Applications of probability graphs in mineral exploration.” *Spec. vol. 4, Association of Exploration Geochemists* (1976), 95 pp”

Sinclair A.J. “Selection of threshold values in geochemical data using probability graphs.” *J. Geochem*. Explor (1974), 3, 129-149.

Sinclair A.J. “Statistical interpretation of soil geochemical data. In: Exploration geochemistry: design and interpretation of soil surveys.” *W.K. Fletcher, S.J. Hoffman* (1986).

Voltattorni, N., Lombardi S. and Rizzo S. ^{222}Rn and CO_2 soil gas geochemical characterization of thermally altered clays at Orciatico (Tuscany, Central Italy). Applied Geochemistry 25(8) (2010):1248–1256

Wolery T.W., Jarek R.L. “Software user’s manual. EQ3/6, Version 8.0. Sandia National Laboratories – U.S. Dept. of Energy Report (2003).”

Wolery T.W., Jove-Colon C. “Qualification of thermodynamic data for geochemical modeling of mineral-water interactions in dilute systems.” *Sandia National Laboratories* (2007) Report ANL-WIS-GS-000003 REV 01.